RSC Advances

PAPER

View Article Online
View Journal | View Issue

Cite this: *RSC Adv.*, 2015, **5**, 56993

Mechanism of enhancement in NH_3 sensing for surface functionalized WO_3 film

Vibha Srivastava†* and Kiran Jain

Received 10th June 2015
Accepted 24th June 2015

DOI: 10.1039/c5ra11050e

www.rsc.org/advances

Sensors were fabricated using a screen-printing technique using WO_3 produced by a sol–gel process. Surface functionalization was achieved by using normal and catalyzed SiO_2 coatings. The variation of sensor response to ammonia gas was investigated for both undoped and platinum doped WO_3 sensor layers. The response to ammonia exhibited significant improvement following surface modification with catalyzed silica. The increase has been attributed to an increase in Schottky barrier height.

Introduction

Metal oxide semiconductor based sensors offer nondestructive, continuous and rapid measurement of low concentrations of gases. Many oxides such as ZnO, SnO_2, In_2O_3, WO_3 *etc.* have been extensively investigated. These oxides are non-stoichiometric and free electrons originating from oxygen vacancies contribute to electronic conductivity. The detection of a change in resistance on exposure to gas is the working principle of these sensors. Since the surface layer of the material is mainly involved in these reactions, the gas response is strongly dependent on the surface to volume ratio.[1]

Detection of ammonia at lower levels is important for many fields of technological importance such as food technology, chemical engineering, medical diagnosis, environmental protection and monitoring of vehicle interiors.[2] Increased pollution awareness has increased the demand for sensors for continuous monitoring as exposure to high ammonia concentrations is a serious health threat. Tungsten oxide is n-type semiconductor with an interesting photoconductivity and resistivity which has been shown sensitive to low concentration of NH_3 and NO_x.[3] To further improve the gas response, noble metals are added to the sensing layer to enhance the catalytic reaction with the target gases.[4,5] Gas sensing involves adsorption induced changes on the surface thereby sensor response can be controlled by surface functionalization of the semiconductor oxides.[5] To improve gas selectivity in oxide sensors, bilayer configuration of sensing layers is often used.[6,7] A thin permeable membrane of SiO_2 has been shown to increase gases sensitivity, selectivity and high temperature stability.[8,9] We have shown that Pt doped WO_3 with SiO_2 is highly sensitive to NH_3 at 450 °C in comparison to Au and Pd doped WO_3 with and without SiO_2 overlayer.[10] SiO_2 membrane with a thickness gradient had been applied on gas sensor arrays to achieve different gas sensitivities for individual sensor elements. Such arrays have been employed for electronic nose applications using pattern recognition methods.[11] La_2O_3–Au/SnO_2 – layer with silica coating is used in CO sensor.[12] High ammonia sensitivity is reported for SnO_2 coated with Pt and SiO_2.[13] We have shown a significant improvement in ammonia sensitivity of WO_3 thick films by coating with a platinum catalyzed silica–niobia layer leading to sensors capable of detecting ammonia down to 15 ppm.[14,15] In the present work, we investigate electrical property of SiO_2 and Pt/Nb/SiO_2 coated undoped and Pt doped WO_3 powder to understand the role of surface functionalization layer.

Experimental

The WO_3 powder is prepared by adding 5 gm of tungstic acid powder to 30% H_2O_2. The mixture is then stirred for 8 h to obtain peroxotungstic acid gel (PTA) and further dried to obtain precursor powder of WO_3. This powder is calcined at 600 °C for 4 hours in air to obtain tungsten oxide powder.[14] Pt doped powder is prepared by adding WO_3 powder to a solution of 0.4 wt% chloroplatinic acid in water before drying. A simple traditional design is used to fabricate metal oxide sensor which consists of alumina substrate with a printed heater and a gold finger electrodes. Thick film pastes were prepared and screen printed of pure undoped WO_3 powder (W) and Pt doped WO_3 powder (W/Pt). After drying at 120 °C for 30 minutes, sensors were fired at 800 °C for 10 minutes in a furnace. The thickness of WO_3 layer was around 50 μm. For surface functionalization with silica, a sol was prepared using tetraethyl *ortho*-silicate (TEOS), hydrochloric acid and ethanol. A drop of this sol was dropped on W and W/Pt sensors, dried and fired at 600 °C resulting in silica coated (W/S and W/Pt/S) samples. Another sol was prepared for catalyzed silica sol coating, for which 0.1 gm niobium chloride was dissolved in 10 ml ethanol, to which 0.1 gm platinum chloride powder was added, four drops of this

Physics of Energy Harvesting, National Physical Laboratory, Dr. K. S. Kishnan Marg, New Delhi, India-110012. E-mail: vibhasri15@gmail.com; v.srivastava@lancaster.ac.uk
† Present address: Lancaster University, Lancaster, UK-LA1 4YB.

Pt/Nb sol were mixed with one drop of silica sol and finally one drop of this sol was coated over the sintered WO_3 sensor. The surface coatings was dried at 120 °C for 30 minutes and then fired at 600 °C for 10 minutes. This resulted in catalyzed silica sensors (W/C and W/Pt/C). The annealing temperature for the surface layers is kept lower than the sintering temperature to avoid undesirable changes in the microstructure of WO_3. However at firing temperatures, SiO_2 and catalyzed SiO_2 coated on the surface of WO_3 may penetrate/diffuse to the grain boundary which is confirmed by change in Schottky barrier height.

Resistance of the sensors is measured using a Keithley 2000 multi-meter in static ambient. The sensors were fitted onto a sample holder which can be heated externally. The temperature of the films is determined by a thermocouple attached nearer to the sensor and was kept constant during each measurement. The measurements were first performed at each temperature in air at room environment and then a required amount of NH_3 was added to the chamber (volume 350 cm^3) through a rubber septum using a syringe. Sensor response (S) is generally defined as the ratio of the resistance in dry air (R_{air}) to that in presence of ammonia (R_{gas}), *i.e.* $S = R_{air}/R_{gas}$. Different ammonia concentrations were obtained by successive injections, after measurement at the highest concentration (4000 ppm) the test chamber was flushed with dry air. Estimation of crystallite size, phase and crystalline planes was carried out using a Technai G2 electron microscope operated at 200 kV accelerating voltage. For TEM measurement of sensor samples after surface functionalization were removed from alumina, sonicated in water to make dilute dispersion and a drop of this dispersion is put over carbon coated grid. XRD pattern of the sample is acquired by a Bruker D8 Advance X-ray diffractometer (Germany) using Cu Kα radiation ($\lambda = 0.154178$ nm).

Results and discussion

XRD and TEM analysis is carried out to ascertain crystalline quality of WO_3 powder which calcined at 600 °C for 4 hours. XRD pattern of WO_3 powder is shown in Fig. 1 and the TEM image of silica coated WO_3 sensor is shown as an inset. XRD pattern is indexed by comparing it with standard patterns [JCPDS 43-1035] suggests that the powder is crystallized as WO_3 with monoclinic structure whose lattice parameters $a = 0.73$, $b = 0.75$ and $c = 0.77$ nm are in good agreement.[16,17] No other peaks related to tetragonal/orthorhombic phase are observed. The lattice fringes present in the polycrystalline grains of WO_3 (TEM image of SiO_2/WO_3 is shown as an inset) further confirm monoclinic phase. Thus silica has no effect on the crystalline nature of WO_3.

The surface coverage of silica and platinised/niobium silica coating over WO_3 film is ascertained by TEM measurement. Plan view TEM image of silica and platinised/niobium silica coating over WO_3 film is shown in Fig. 2(a). An envelope of 20–50 nm wide SnO_2 layer is seen over 30–50 nm sized WO_3 grains. Since the silica over-layer is few nanometers thick it partially covers WO_3 grains. The magnified plan view TEM image of silica and platinised/niobium silica coating over WO_3 film is shown in Fig. 2(b). In TEM image 30–50 nm wide discontinuous sheets of SnO_2 can be seen over WO_3 layer along with Pt (2–5 nm) catalysts dispersed over WO_3. EDX pattern (not shown here) confirms presence of Pt, Nb, Si and O_2. The selective area diffraction (SAD) pattern (not shown here) confirms polycrystalline nature of WO_3.

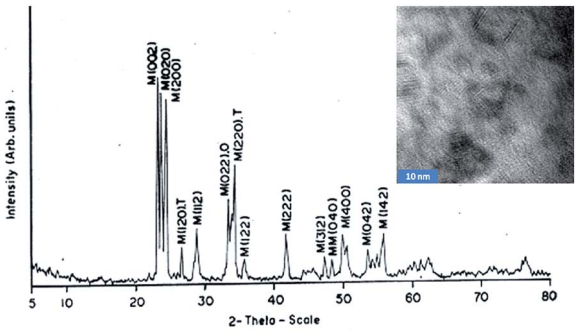

Fig. 1 XRD pattern of WO_3 powder with TEM image of silica coated WO_3 sensor as an inset.

Response was measured at different temperatures from 200 to 450 °C. The response was very low at temperatures below 200 °C and increased with increasing temperature. The effect of surface functionalization over WO_3 is shown in Fig. 3(a), which shows the gas response at a concentration of 4000 ppm ammonia for the as prepared (W), silica coated (W/S) and catalyzed silica (W/C) sensors at different temperatures. Fig. 3(b) shows the gas response at different concentrations of ammonia at 450 °C. The response to ammonia was enhanced after SiO_2 coating and improved further after catalyzed silica coating. Fig. 3(c) shows the gas response for Pt doped WO_3 after surface functionalization with SiO_2 and catalyzed SiO_2 coatings at different temperatures for 4000 ppm ammonia. Pt doped sample shows higher response to ammonia as compared to undoped sample in all cases investigated. Surface functionalization with SiO_2 as well as catalyzed silica coating, increased the gas response for Pt doped as well as undoped sensor. Highest gas response was observed at 350 °C for Pt doped sample after the catalyzed silica coating. Fig. 3(d) shows the gas response for different concentrations of ammonia at 350 °C. Noble metals or oxides of other elements added to the sensor surface provide sites for adsorption which promotes (or inhibit) surface

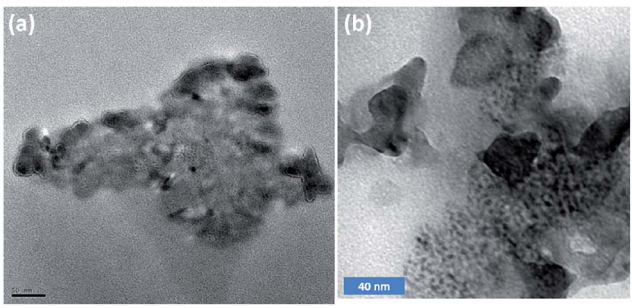

Fig. 2 Plan view TEM image of (a) silica and platinised/niobium silica coating over WO_3 film and (b) magnified TEM image.

catalysis and surface electronic states. As a result, gas sensitivity, response time and selectivity can be dramatically improved. To understand the improvement caused by functionalization layer over WO_3, and the role of the top layer, we measured the resistance of all WO_3 samples as a function of temperature. The samples were first heated at 450 °C for one hour to promote desorption of any pre-adsorbed gases from the atmosphere as well as moisture. The resistance was than measured by reducing the temperature continuously.

Fig. 4(a) and (b) show $\ln(R)$ *vs.* $(1/T)$ curve for undoped and Pt doped sample, before and after surface functionalization with SiO_2 and catalyzed SiO_2. The resistance of all the samples increases on decreasing temperature with two different slopes. Significant increase in resistance of the sensor material was observed after doping with Pt, as well as after coating with silica and catalyzed silica. The resistance in air at 300 °C for undoped WO_3 was 0.29 M ohm, which increased to 1.2 M ohm and 1.6 M ohm after silica and catalyzed silica coating respectively. Similarly, the resistance in air at 300 °C for Pt doped sensor was 0.69 M ohm, which increased to 2.15 and 5.4 M ohm after silica coating and catalyzed silica coating respectively.

It is generally accepted that the charged species such as O^-, O^{2-} are adsorbed on the metal oxide surface in air. The reducing gas (NH_3) reacts with oxygen adsorbed on the surface of the sensor as[3]

$$R + O_{ads}^{-} \leftrightarrow RO + e^{-} \quad \text{(i)}$$

To maintain charge neutrality, the electrons are released back into WO_3, resulting in an increase of electron concentration and the decrease of the resistance. According to this model of metal oxide gas sensor, since the material is polycrystalline, the conductivity of a sensor is dominated by the Schottky type potential barrier that develops at the inter grain boundaries of the film in the presence of surface oxygen.[18] An alteration of the

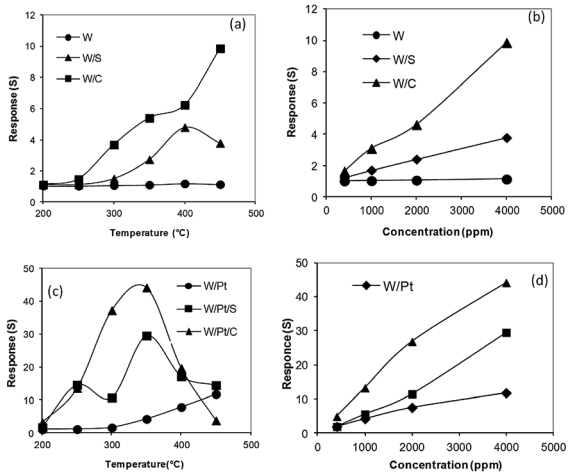

Fig. 3 Sensor response for undoped WO_3 (a) at different temperatures for 4000 ppm ammonia (b) different concentrations of ammonia at 450 °C, sensor response for Pt doped WO_3 (c) at different temperatures for 4000 ppm ammonia (d) different concentrations of ammonia at 350 °C.

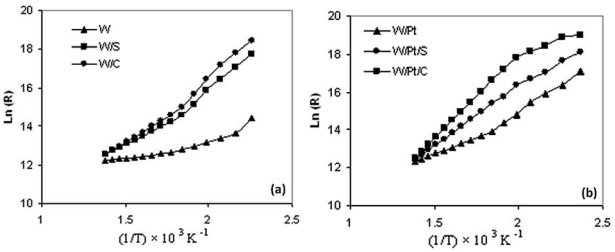

Fig. 4 $\ln(R)$ *vs.* $(1/T) \times 10^3$ curve for (a) undoped WO_3 and (b) Pt-doped WO_3.

of the electron concentration in the grain due to the presence of gas that reacts with oxygen adsorbates leads to a modification of the potential barrier height, which results in a change in conductivity. According to this model, the conductivity is expressed as

$$G = G_0 \exp(-E_b/kT) \quad \text{(ii)}$$

where E_b is the barrier height at intergranular contacts, which is proportional to adsorbed oxygen ion concentration, and G_0 a factor including the bulk conductance.[19] The Schottky barrier height E_b was determined, between 200 to 450 °C temperature range, for all the samples using Fig. 3 and 4. Table 1 shows the Schottky barrier height for all sensor samples. The Schottky barrier height for undoped sensor was 0.14 eV which increased to 0.28 eV after Pt doping. The functionalization with silica and catalyzed silica coatings increased the barrier height to 0.36 eV and 0.44 eV for undoped WO_3 sensor; and 0.56 and 0.78 eV for Pt doped WO_3 sensor.

The increased performance of the present sensors can be understood in terms of the existing models developed for SnO_2 sensors.[20] In case of Pt doped WO_3 sensor, the chemical sensitization mechanism might be assumed to operate for Pt catalyst. Platinum nanoparticles catalytically activate the dissociation of oxygen or ammonia. The increase in gas sensitivity due to Pt doping can be ascribed to spill over of the atomic oxygen formed catalytically on the Pt particles that migrate into the WO_3 and the back spill over effect in which the weakly bound molecular oxygen migrate to the Pt. As a result both the delivery of active species to and from WO_3 surface was promoted by catalytically active Pt nanoparticles. This is reflected as an increase in the barrier height after Pt doping (W/Pt) as shown in Table 1. Further, the resistance measurements show that the addition of catalytic Pt induces an increase in the resistance of WO_3 film.

Table 1 Schottky barrier height for different WO_3 sensors

Sample	Barrier height (eV)
W	0.14
W/S	0.36
W/C	0.44
W/Pt	0.28
W/Pt/S	0.56
W/Pt/C	0.78

An increase in the Schottky barrier height was observed after surface functionalization with silica as well as catalyzed silica coating. The response or recovery time had not increased after surface functionalization. This indicates a catalytic role of the surface functionization layers. Earlier studies on SnO_2 have shown that SiO_2 has no catalytic activity individually but and can enhance the activity of other catalysts.[13] Thin films of SiO_2–WO_3 composites were reported to be more sensitive to NO_2 than pure WO_3 films due to the decreased grain size and increased porosity.[21] In the present work, the silica coating was fired at a lower temperature (600 °C) as compared to the sensor layer sintering temperature (800 °C), change in the microstructure is not likely. Increased resistance in air at 250–450 °C after surface functionalization with silica as well as catalyzed silica (Pt/Nb/SiO_2) was observed. This increase in resistance can be explained by considering the electronic interaction between WO_3 and phases existing at the grain boundaries. After surface functionalization with silica or catalyzed silica coating, the top layer consisting either of silica or of Pt, silica and niobia, will diffuse to the grain boundaries of porous WO_3 layer during firing. This may modify the grain boundary properties as reflected in enhanced Schottky barrier height that causes enhancement in response magnitude.

In metal oxides the surface oxygen species with a negative charge and metal cations play the role of Lewis basic and acidic centers respectively. Ammonia molecule behaves as a strong Lewis base and preferentially adsorbs at acid centers. For SnO_2 sensors, the sensitivity for ammonia was found to increase with the density of acid centers.[22] A similar enhancement in ammonia sensitivity can be expected with an increase in acid centers at WO_3 surface. Niobium oxide is a solid acid with high acidity on the surface.[21] Nb_2O_5 can be deposited on silica to form stable surface oxide phase. Nb_2O_5 is well dispersed on SiO_2 by interaction of the sylanol group of SiO_2 with niobium precursor forming Nb–O–Si bonds and surface niobia possesses a considerable amount of acid sites.[23,24] It is proposed that WO_3–Nb_2O_5 is a solid with strong acidity based on Bronsted acid sites on the surface[22,25] due to substitution of pentavalent niobium for hexavalent tungsten in the lattice of tungsten oxide. The dopant niobium is an acceptor leading to decreased electron concentration at the grain boundary region when substituted for tungsten. This results in an increase in acid sites when Nb_2O_5–SiO_2 exists at WO_3 grain boundaries. Our results of enhanced ammonia response in sensors with catalyzed silica coating can be attributed to the presence of increased acidic sites for ammonia oxidation. As the results indicated, functionalization with silica was also effective in enhancing the Schottky barrier height, however the highest barrier was observed for catalyzed silica coating on Pt doped WO_3, which showed maximum gas response. This is reflected as the increase in barrier height in as more oxygen ions can be adsorbed in air. This enhanced barrier height in other way reflects trapping of higher concentration of electrons and hence enhanced resistance due to decrease in current carrier. On exposure to ammonia gas, ammonia reacts with adsorbed oxygen at surface and these trapped electrons are released back, that increases the conductivity.

Conclusions

In conclusion, the NH_3 sensing properties of the WO_3 thick film have been significantly improved by addition of catalyzed silica overlayer onto the WO_3 film surface. A possible mechanism of surface functionalization on the sensing properties is explored. The increased gas response was correlated to increased barrier height and increased air resistance. The increased gas response can be explained through an increased Schottky barrier height due to increased acidic sites attributed to the replacement of hexavalent tungsten by pentavalent niobium at the grain boundaries.

Acknowledgements

We are thankful to Mr Y. K. Jain, CEERI Pilani for providing the sensor substrates. We are also thankful to Dr K. N. Sood and Dr S. K. Halder for measurement of SEM and XRD. One of the authors (VS) thanks Council of scientific and industrial research for the award of Research Associateship.

References

1 M. Schweizer-Berberich, S. Strathmann, U. Weimar, R. Sharma, A. Seube, A. Peyre-Lavigne and W. Göpel, *Sens. Actuators, B*, 1999, **58**, 318–324.
2 B. Timmer, W. Olthuis and A. van-den-Berg, *Sens. Actuators, B*, 2005, **107**, 666–677.
3 B. T. Marquis and J. F. Vetelino, *Sens. Actuators, B*, 2001, **77**, 100–110.
4 M. Penza, C. Martucci and G. Cassano, *Sens. Actuators, B*, 1998, **50**, 52–59.
5 A. Kolmakov, D. O. Klenov, Y. Lilach, S. Stemmer and M. Moskovits, *Nano Lett.*, 2005, **5**, 667–673.
6 V. A. Chaudhary, I. S. Mulla and K. Vijayamohanan, *Sens. Actuators, B*, 1999, **55**, 154–160.
7 R. S. Niranjan, S. D. Sathaye and I. S. Mulla, *Sens. Actuators, B*, 2001, **81**, 64–67.
8 C. Pijolat, J. P. Viricelle, G. Tournier and P. Montmeat, *Thin Solid Films*, 2005, **490**, 7–16.
9 C. O. Park, S. A. Akbar and J. Hwang, *Mater. Chem. Phys.*, 2002, **75**, 56–60.
10 V. Srivastava and K. Jain, *Sens. Transducers J.*, 2010, **117**, 120–128.
11 J. Goschnick, M. Frietsch and T. Schneider, *Surf. Coat. Technol.*, 1998, **108–109**, 292–296.
12 K. Fukai and S. Nishida, *Sens. Actuators, B*, 1997, **45**, 101–106.
13 Y. D. Wang, X. H. Wu, Q. Su, Y. F. Li and Z. L. Zhou, *Solid-State Electron.*, 2001, **45**, 347–350.
14 V. Srivastava and K. Jain, *Sens. Actuators, B*, 2008, **133**, 46–52.
15 T. D. Senguttuvan, V. Srivastava, J. S. Tawal, M. Mishra, S. Srivastava and K. Jain, *Sens. Actuators, B*, 2010, **150**, 384–388.
16 S. Pokhrel, C. E. Simion, V. S. Teodorescu, N. Barsan and U. Weimar, *Adv. Funct. Mater.*, 2009, **19**, 1767–1774.
17 S. Pokhrel, J. Birkenstock, M. Schowalter, A. Rosenauer and L. Mädler, *Cryst. Growth Des.*, 2010, **10**, 632–639.

18 H. Windischmann and P. Mark, *J. Electrochem. Soc.*, 1979, **126**, 627–633.
19 L. Dae-Sik, H. Sang-Do, H. Jeung-Soo and L. Duk-Dong, *Sens. Actuators, B*, 1999, **60**, 57–63.
20 N. Yamazoe, Y. Kurokawa and T. Seiyama, *Sens. Actuators*, 1983, **4**, 283–289.
21 X. Wang, G. Sakai, K. Shimanoe, N. Miura and N. Yamazoe, *Sens. Actuators, B*, 1997, **45**, 141–146.
22 V. V. Kovalenko, A. A. Zhukova, M. N. Rumyantseva, A. M. Gaskov, V. V. Yushchenko, I. I. Ivanova and T. Pagnier, *Sens. Actuators, B*, 2007, **126**, 52–55.
23 M. Hino, M. Kurashige and K. Arata, *Catal. Commun.*, 2004, **5**, 107–109.
24 P. A. Burke and E. I. Ko, *J. Catal.*, 1991, **129**, 38–46.
25 A. C. S. Lino, M. S. P. Francisco, Y. Takahata and Y. Gushikem, *J. Mol. Struct.: THEOCHEM*, 2005, **724**, 15–17.